United Aircraft Research Laboratories

UNITED AIRCRAFT CORPORATION

EAST HARTFORD, CONNECTICUT

F-910093-38

Investigation of Gaseous Nuclear Rocket Technology

Quarterly Progress Report No. 17
September 16, 1967 through December 15, 1967
Contract NASw-847

REPORTED BY G. H. McLafferty
G. H. McLafferty

DATE December 30, 1967

NO. OF PAGES 26

COPY NO. 11

Report F-910093-38

Investigation of Gaseous Nuclear Rocket Technology

Quarterly Progress Report No. 17 - September 16, 1967 through December 15, 1967

Contract NASw-847

SUMMARY

Work on the fifth year of the program being carried out to investigate gaseous nuclear rocket technology was initiated on September 16, 1967. This investigation covers work in the following technical areas: experimental investigations of the fuel retention characteristics of a model of a coaxial-flow gaseous nuclear rocket; experimental investigations of vortex flow, primarily in an RF-heated vortex, to obtain information for application to a nuclear light bulb reactor; measurements of the opacity of seeds which might be employed in gaseous nuclear rockets; in-reactor measurements of the transmission characteristics of transparent materials; and studies of the effect of the results of these investigations on the characteristics of full-scale engines. In the coaxial-flow tests during this quarter, experiments were conducted to determine the effect of buffer layer velocity and chamber length-to-diameter ratio on containment characteristics. RF vortex tests were conducted to determine the effect of various parameters on the radius of the gas discharge region. Various refinements were made in the equipment for measuring gas opacity, including modifications necessary for determining the opacity of uranium gas. Preparations were initiated for additional tests of transparent materials in a TRIGA reactor.

The investigation described herein is being carried out under Contract NASw-847 with the National Aeronautics and Space Administration through the Space Nuclear Propulsion Office.

COAXIAL-FLOW GNR MODEL TEST PROGRAM

The coaxial-flow jet experiments were continued using the flow visualization and inner-jet gas concentration measurement techniques described in Quarterly Progress Report Nos. 15 and 16 and in Ref. 1. A sketch of the coaxial-flow test apparatus is presented in Fig. 1. The primary objective of recent experiments has been to determine the flow conditions necessary to prevent recirculation downstream of the inner-jet injection location. Results discussed in Quarterly Progress Report No. 16 (see Fig. 3 of that report) indicated that flow conditions with recirculation were accompanied by a substantial decrease in the amount of inner-jet gas contained within the chamber. During this report period, additional flow visualization tests and inner-jet gas concentration measurements have been made for configurations having inlet radius ratios of $r_I/r_o = 0.5$ and 0.7 and chamber length-to-diameter ratios of $L_N/D = 0.75$, 1.0, and 1.25 (see Fig. 1 for nomenclature). The inner-jet gas concentration data from these tests are presently being reduced; the results of the flow visualization tests for $r_I/r_o = 0.5$ will be discussed in this progress report.

An error introduced by the filters in the light absorption equipment used in the inner-gas concentration measurements was uncovered and appropriate corrections were made to the inner-jet concentration data reported in Quarterly Progress Report No. 16. As a result of the error, the previously reported inner-jet gas concentrations for radius ratios less than $r/r_o = 0.3$ were less than the actual concentrations. Although the gas concentration profiles were distorted, the corrected integrated containment results were approximately equal to those previously reported because of the small volume involved (the volume inside $r/r_o = 0.3$ is only 9 percent of the total volume of the chamber). Correction factors for use in the data reduction procedure have been obtained by calibrating the chordal light absorption system in place. This was done by measuring the light transmitted with iodine vapor filling the chamber completely and without iodine present.

Effects of Buffer Layer on Containment of Inner-Jet Gas

Flow visualization studies of buffer gas velocity containment characteristics indicated that large changes occurred in the total amount of inner-jet gas contained in the chamber for tests with the inlet configuration having $r_I/r_o = 0.50$ and $r_B/r_o = 0.65$. The greatest effect occurred for conditions where V_{BAO}/V_I was the maximum value for which recirculation could be prevented by proper choice of buffer gas velocity. Typical photographs from these tests are shown in Fig. 2. The average velocity of the buffer and outer stream and the velocity of the inner jet were constant for these tests. The buffer velocity, V_B, was varied from the outer stream velocity, V_O, to zero; that is, it was varied such that $V_B/V_{BAO} = V_O/V_{BAO} = 1.0$ to $V_B/V_{BAO} = 0$. The best velocity ratio for this configuration was $V_B/V_{BAO} = 0.4$.

As shown in Fig. 2, an increase of V_B/V_{BAO} to 0.55 or a decrease to 0.3 decreased the observed amount of inner-jet gas contained within the chamber.

Results from the inner-jet gas concentration measurements verified the effects shown in Fig. 2. Variations of the average partial pressure ratio of the inner-jet gas in the chamber with V_B/V_{BAO} are presented in Fig. 3 for V_{BAO}/V_I = 9 and 18 with an inner jet of air and for V_{BAO}/V_I = 18 with an inner jet of Freon-11. These results were also obtained with an injection configuration having r_I/r_o = 0.5 and r_B/r_o = 0.65, a chamber length-to-diameter ratio of L_N/D = 1.25, and an exhaust nozzle diameter of 6 in. at the throat. Preliminary results of tests with an injection configuration having r_I/r_o = 0.7 and r_B/r_o = 0.8 indicate much less effect of buffer velocity on the inner-jet containment characteristics than shown in Figs. 2 and 3.

Effects of Chamber L_N/D on Maximum V_{BAO}/V_I Without Recirculation

The effect of chamber L_N/D on the maximum value of V_{BAO}/V_I for which recirculation could be prevented by proper choice of the buffer velocity was determined by flow visualization tests with inner-jet gases of Freon-11 and air. The configuration employed for these tests had inlet radius ratios of r_I/r_o = 0.5 and r_B/r_o = 0.65 with an exhaust nozzle throat diameter of 6 in. For tests with Freon-11 as the inner-jet gas, the maximum ratio of V_{BAO}/V_I for which recirculation could be prevented varied from 39 for L_N/D = 0.75 to 19 for L_N/D = 1.25 (Fig. 4). The ratio of V_B/V_I required to prevent recirculation at the maximum ratio of V_{BAO}/V_I are also shown in Fig. 4. The highest value of V_B/V_I = 16 was obtained for L_N/D = 1.0. The ratio V_B/V_{BAO} varied from 0.3 to 0.5, with the maximum value for L_N/D = 1.0. The maximum velocity ratios V_{BAO}/V_I and V_B/V_I for the test with air as the inner-jet gas were approximately equal to half those for tests with Freon-11 as the inner-jet gas. However, the variation of velocity ratio V_B/V_{BAO} with L_N/D was approximately the same.

FLUID MECHANICS OF NUCLEAR LIGHT BULB REACTOR

Results of Tests Employing the 1.2-Megw RF Induction Heater

The primary objective of the tests conducted during this report period was to investigate the factors that determine the size and power deposited in confined radio-frequency gas discharges at pressures on the order of 1 atm in flowing systems. A second objective was to develop experimental techniques at low power levels which can be used in future tests at high power levels. Several different geometric configurations were employed. Sketches of the three principal configurations which were used are presented in Figs. 5, 6, and 7 along with photographs of typical discharges. These configurations are designated: (1) simple gas load configuration, (2) simple gas load configuration with swirl injection, and (3) vortex configuration.

Tests With Simple Gas Load Configuration

The simple gas load configuration shown in Fig. 5a consists of two coaxial, thin-walled fused silica tubes. The gas discharge occurs in the region within the inner tube. Cooling water for the inner tube flows through the annular space between the inner and outer tubes. Tests were conducted without any flow of gas through the inner tube and with axial flow.

In the tests without flow, the discharge was started at an inner tube pressure of 5 mm Hg abs. Increases in tube pressure were accomplished by admitting argon until the desired pressure level was obtained and then subsequently shutting off the argon flow. Tests were conducted at inner tube pressures from 0.5 to 1.5 atm and discharge power levels from approximately 2 to 5 kw. Figure 5b is a photograph showing the type of discharge obtained in these tests. For this discharge, the pressure was 1.5 atm; however, the shape of the discharge region was similar at all pressures. The discharge region was not symmetrical about the centerline of the inner tube but occupied a region toward the top of the inner tube. This is believed to be due to buoyancy effects; the tube was oriented with its centerline horizontal.

In the tests with axial flow, the inner tube pressure was again reduced to 5 mm Hg abs and the discharge was started. The axial flow of argon gas was then started. It was extremely difficult to obtain a steady discharge; in most tests, the discharge oscillated in both the radial and axial directions. The radial oscillation resulted in heating of the inner tube wall due to the presence of the discharge near the wall. Buoyancy effects were also noted in these tests.

Tests With Simple Gas Load Configuration With Swirl Injection

It was expected that swirl flow would provide the radial force necessary to

counteract the buoyancy effects in the discharge and thereby provide improved confinement. The simple gas load configuration was modified as shown in Fig. 6a to include provision for injection of argon gas with swirl (i.e., with both tangential and axial components of injection velocity).

Steady discharges were obtained using argon gas at pressures up to 1.5 atm. A photograph of a typical argon discharge is shown in Fig. 6b. Lines indicating the location of the inner tube wall are shown. The discharge was symmetrical about the centerline; thus, the swirling flow appears to have overcome the buoyancy effects. The diameter of the discharge region as measured from the photograph in Fig. 6b was approximately 0.7 times the inside diameter of the inner tube. By adding more axial flow to the swirl flow, it was possible to control the axial location of the discharge region. Discharges that were approximately symmetric with respect to the heater coils were produced in this manner.

One factor which limited the power that could be deposited in the discharge in tests employing the simple gas load configuration with swirl was severe heating of the inner tube several inches downstream of the heater coils. This heating may have been caused by mixing of the hot gas core with cooler gas near the wall. A water-cooled copper end wall having a 0.75-in.-dia port at its center was placed immediately downstream of the discharge region. In one test using this end wall with helium as the flowing gas, approximately 16 kw were deposited in the discharge with little resultant wall heating. The helium weight flow rate was 31.4×10^{-4} lb/sec and the discharge diameter was approximately 0.6 times the inside diameter of the inner tube in this test.

Tests With Vortex Configuration

Upon completion of the preliminary tests discussed previously, the vortex configuration shown in Fig. 7a was installed. This configuration has a 2.28-in.-ID, water-cooled inner tube and 1.75-in.-dia water-cooled copper end walls. The end walls were 6 in. apart and had 0.3-in.-dia thru-flow ports. Argon was injected with swirl through 6 tubes located at the periphery of one end wall (see Fig. 7a). Tests were conducted with argon gas at inner tube pressures as high as 1.95 atm.

A typical discharge is shown in Fig. 7b. The weight flow rate of argon was varied from 2.9×10^{-3} lb/sec to 16.0×10^{-3} lb/sec. The power deposited in the discharge varied from 4.8 kw to 22.6 kw. The diameter of the discharge was changed by varying the argon weight flow rate. The discharges were approximately symmetrical with respect to the heater coils. Discharges having diameters from 0.25 to 0.75 times the inside diameter of the inner tube were obtained. Tests of this configuration will be continued during the next report period.

Transparent-Wall Model Designs

Design of transparent-wall model configurations for use in the 1.2-megw RF induction heater was initiated during this report period. Sketches of two

preliminary model designs are presented in Fig. 8. Figure 8a shows a design having axial coolant tubes and three rows of injection tubes to drive the vortex. Figure 8b shows a more complex design having circumferential coolant tubes as well as injection tubes to drive the vortex. Also presented in Fig. 8 is a table of present and future specifications applicable to transparent-wall model designs. Specifications listed for the present models have been eased relative to those that would be required for a full-scale nuclear light bulb engine to facilitate fabrication of models for use in the initial tests.

Particle Seeding Experiments

Preliminary studies of particle seeding methods for injecting tungsten or other seed materials into a plasma have indicated that there are three primary problems to overcome before an adequate system can be developed. These problems are (1) to finely disperse the particles (deagglomeration), (2) to obtain a uniform flow of particles (minimize or eliminate random slug flow), and (3) to obtain the highest weight flow rate of particles for a given carrier gas weight flow rate.

Preliminary particle seeding experiments using sub-micron tungsten powder (0.02 to 0.06 microns) and argon as the carrier gas were conducted using one of the Research Laboratories' commercial screw-driven powder feeders. Fine dispersion and uniform flow of the tungsten particles could not be obtained with this device. Also, during some tests, packing of the particles around the rotating feed screw occurred which completely stopped the flow of particles from the feeder.

Further experiments were directed toward investigating techniques by which the particles could be finely dispersed (deagglomerated). It was found that this could be accomplished by flowing the particles through a pneumatic atomizing nozzle (a conventional paint spray nozzle). Particle weight flow rates up to approximately 2×10^{-3} lb/sec were obtained in some of these preliminary experiments.

A complete particle seeding system is now being assembled using this dispersion technique. A schematic of this system is shown in Fig. 9. In order to insure a uniform flow rate of particles, it will be necessary to prevent large agglomerates from entering the dispersal nozzle. The rotating fan blades in the powder storage cannister (Fig. 9) will constantly agitate the particles and should minimize agglomeration. Tests to determine the operating characteristics of the particle seeding system will be conducted during the next report period.

Technical discussions concerning the particle feeding problems were conducted at Georgia Institute of Technology with Professor Clyde Orr and Mr. Edward Y. H. Keng. Several helpful ideas were obtained which were incorporated in the design of the particle seeding system.

OPACITY MEASUREMENTS IN HIGH-TEMPERATURE GAS VORTEXES

Vortex Flow Conditions

As part of the Company-sponsored research program, modifications were made to the 80-kw RF induction heater to provide better coupling between the plasma load and the RF generator. Early in this report period the coaxial resonator that was employed in all previous tests (see Fig. 2 of Quarterly Progress Report No. 13-U) was replaced with a six turn coil. A temporary tunable coupling network was installed between the power amplifier and the coil. The power amplifier was converted from grounded grid to grounded cathode and the self excitation was replaced with a driven oscillator. The gas load was converted from a vortex type flow to a straight pipe flow. Initial tests with this modified configuration resulted in an improved gas discharge that was steady and confined away from the walls of the fused silica tube. Photographs of the discharge using two different film exposures are presented in Fig. 10.

These temporary modifications appeared so desirable that the facility was shut down so that necessary new components could be purchased and permanently installed. This installation has been completed under the Corporate-sponsored program and testing with gas discharges has been resumed. Initial tests resulted in up to 20 kw of power deposited in the gas with an efficiency (defined as power into the gas divided by d-c plate power) of 40 percent. Since the system was not fully tuned for these tests, it is expected that the efficiency will increase when the system is fully tuned. In a subsequent test, 11.5 kw of power was deposited in the gas with a corresponding efficiency of 60 percent. The best performance resulted when a small amount of swirl was added to the gas flow to stabilize the discharge.

Design of various components required for measurement of spectral emission data were undertaken during this quarter. Among these components were 1) a discharge tube that will permit the emitted radiation to pass directly into the monochrometer without passing through either fused silica walls or air, thus allowing spectral emission data to be obtained in the ultraviolet and infrared regions of the spectrum, and 2) a disposable condensing system for the exhaust which will permit use of uranium compound seeds in the gas discharge.

Spectral Measurements

An appraisal of the tungsten spectral data obtained to date in the 80-kw RF heater has led to the conclusion that many more significant spectral lines exist in the ultraviolet than in the infrared wavelength range. In order that the maximum data on line intensities be available for comparison with theoretical estimates of tungsten emission spectra, attention has been directed toward expediting early use

of the McPherson UV-visible spectrometer which will permit extended observation in the UV.

Activity during this period has been limited to design and fabrication of equipment and ancillary systems. The McPherson spectrograph has been mounted on a modified milling table and an indicating drive system is being attached to furnish lateral motion for scanning of the discharge. (This should provide improved positioning accuracy relative to the system employed in preceding tests.) An EMI 9558 phototube has been purchased for use in temperature surveys of the argon discharge; its special usefulness is the wide range which enables observation of red and blue argon lines without phototube change. Finally, some appropriate modifications based on recent experience are being incorporated into a Corporation-built signal conditioner which will have improved flexibility and performance with respect to signal strength, linearity, and output monitoring. The overall design and fabrication of auxiliary equipment is approximately 80 percent complete, and it is expected that all items will be ready for tests during the next reporting period, at which time the RF spectral absorption measurements will resume.

Spectral Calculations

During the past quarter the line-intensity machine program has been modified to include the requisite atomic data for molybdenum I and molybdenum II. In addition, calculations have been performed to estimate the transition probabilities for approximately 2200 tungsten II lines. (Currently, 107 tungsten II lines are treated in the program.) The line-intensity machine program will be modified to incorporate these tungsten II data. Similarly, calculations of transition probabilities for approximately 1200 uranium I lines are being made. Upon completion of the analysis of transition probabilities for uranium I, the data will be incorporated in the line-intensity program.

RF THEORY

Theoretical calculations were made to investigate gas discharge characteristics in the presence of RF fields. In these calculations, energy was assumed to be deposited in the gas by RF-induced currents and removed by the combined effects of conduction and radiation (the addition of convection terms is presently being considered). Only radial variations of the gas properties and the electromagnetic fields were considered. Variations with temperature of electrical conductivity, thermal conductivity, and gas radiation were obtained from Ref. 2. Some results are presented in Fig. 11 for an argon discharge at a pressure of 1 atm. The variations with radius of the temperature, heat conduction, axial magnetic field, and circumferential electric field are shown for two cases in which the temperature at the centerline was 8000 K and the magnetic field at the centerline was 5.0 amp-turns/cm. The solid curves in Fig. 11 are results obtained with gas radiation present, while the dashed curves do not include gas radiation (i.e., an emissivity of zero). The results show that radiation can markedly effect the heat flux and magnetic field distributions but has less effect on the gas temperature and electric field distributions.

IN-REACTOR MEASUREMENTS OF TRANSPARENT WALL TRANSMISSION

As noted in Refs. 3 and 4, discrepancies have been observed between time constants for decoloration of radiation-induced opacity measured during TRIGA tests and corresponding values measured following Union Carbide tests. As a result, additional in-TRIGA tests will be conducted to attempt to resolve these discrepancies. The optical equipment used in preceding tests to measure the transmittance characteristics of fused silica before, during, and immediately after a TRIGA reactor pulse is presently being set up and bench tested. Several modifications are being incorporated to improve the reliability of the equipment and to reduce the signal increase which has occurred in past tests near the peak of the reactor pulse. For example, additional cooling of the hydrogen lamp is being provided in order to improve the long term stability of the output radiation. The optical radiation from the lamp will also be focused (instead of collimated) into the corner cube specimen located at the internal end of the reactor beam port to provide a greater intensity of optical radiation. This should reduce sample fluorescence (if any) and minimize the signal level increase with respect to the hydrogen source during the reactor pulse. Additional lead shielding around the photomultiplier will also be provided when the equipment is set up at the University of Illinois in January 1968.

Some transmission measurements will be made using specimens which have been pre-annealled at 1050 C for one hour to match the preconditioning process performed upon the specimens used in the post-reactor (Union Carbide) experiments. Unannealled specimens will also be tested to determine if any variation exists due to the specimen preconditioning process. These measurements will be made over a range of temperatures (500 to 900 C). Two wavelengths will be monitored during different tests; one, 2150 Å (the center of the irradiation-induced absorption band), and two, 3000 Å (not associated with an irradiation-induced absorption band).

Two additional types of tests will be performed during the next experimental program at TRIGA which were not included in the previous program. These tests are intended to obtain information concerning any effects of the irradiation pulse on sample fluorescence and temperature gradients. To examine the effects of sample fluorescence on signal level, reactor tests will be made under the same instrument test conditions with the exception that the hydrogen source current will be zero. Any sample fluorescence or radiation within the same spectral band which is the same relative intensity as the hydrogen lamp will be detected. If fluorescence is detected, it will give an explanation for the insufficient bypass correction obtained during the previous tests. These fluorescence tests will be conducted at at least two specimen temperatures.

Schlieren tests will also be performed by photographically recording the output from the sample during the irradiation pulse. Such tests will determine the possible existence of index of refraction gradients caused by thermal gradients within

the specimen. These gradients will cause deviation of the optical beam from the normal optical axis. During normal transmission tests, a displacement of the optical beam at the entrance slit of the monochrometer would result in a reduction of signal level at the photomultiplier causing an apparent loss of transmission. A Milliken high speed camera will be used for the photographic recording at a framing rate of 500 frames per second. These photographic records will necessarily have to be made in the visible region because of the film insensitivity in the ultraviolet. In addition, these photographs will provide a record of any sample motion during the irradiation.

A series of test runs will also be conducted for the purpose of determining the cause of signal level changes during the bypass runs. These tests may be performed prior to the transmission tests if the modifications presently being incorporated into the apparatus are insufficient to remove the signal change in the bypass runs.

ENGINE DESIGN

It was noted in the studies in Ref. 5 that a reduction in U-233 critical mass could be achieved for the reference engine configuration by increasing the mass of moderator in the end walls and by reducing the amount of neutron absorbing materials in the end walls and exhaust nozzle regions. Redesign of the reference configuration was initiated to accomplish both of the indicated changes. Addition of moderator mass to the end walls has been accomplished by a combination of increasing total moderator mass and redistribution of some of the internal moderator materials to the end walls. This also results in more nearly equal power densities in the central and peripheral unit cavities.

The principal contribution to neutron absorption in the lower end wall was from the tungsten struts in each unit cavity which support the hemispherical plug at the end of the fuel region (see Fig. 4 of Ref. 6). These struts have been eliminated by increasing the number of exhaust nozzles per unit cavity from one to three; leading to a total of 21 exhaust nozzles for the entire engine. With this redesign, stacked moderator material would be supported by the pressure vessel at its base and the exhaust nozzles would be non-contiguous penetrations through the lower end wall moderator material. The resulting elimination of tungsten structural support members from the lower end wall region causes a reduction in neutron absorption by a factor of about 10.

The effect of these changes on U-233 critical mass has not been calculated as yet. However, preparation of revised material volume fractions and neutron cross sections has begun.

A digital computer program has been written to integrate the neutron kinetic equations for the nuclear light bulb engine. The equations include fuel injection and loss rates, loss rates of delayed neutron precursors, and reactivity feedback proportional to the variations in nuclear fuel loading with variations in the fuel and delayed neutron precursor time constant. At present, the code can calculate changes in neutron level resulting from step, ramp, or oscillatory variations in either the neutron multiplication factor or the fuel and precursor time constant. A coupled equation which describes variations in pressure across the transparent wall with variations in neutron level has been formulated and is being added to the program.

MISCELLANEOUS

Discussions of one or more phases of gaseous nuclear rocket technology were presented at the following:

October 24, 1967 - U.S.A.F. Aerospace Research Laboratories, Thermomechanics Research Laboratory, Wright-Patterson Air Force Base, Ohio (Dr. Ward C. Roman, Dr. Herbert O. Schrade, and Mr. Paul W. Schreiber).

November 2, 1967 - Georgia Institute of Technology, Engineering Experiment Station, Atlanta, Georgia (Professor Clyde Orr and Mr. Edward Y. H. Keng).

November 11, 1967 - Nuclear Engineering Department at MIT (seminar entitled "Gas-Core Nuclear Rocket Engines")

November 13, 1967 - Atomic Energy Commission Headquarters, Germantown, Maryland (Messrs. D. Gabriel and F. C. Schwenk and Captain C. E. Franklin).

In addition, during the reporting period, the following visited the Research Laboratories and discussed one or more phases of gaseous nuclear rocket technology:

November 26, 1967 - Dr. J. C. Evvard and Mr. R. G. Ragsdale from the NASA Lewis Research Center and Mr. F. C. Schwenk and Captain C. E. Franklin from the Space Nuclear Propulsion Office

December 11, 1967 - Captain C. E. Franklin from the Space Nuclear Propulsion Office and Mr. R. G. Ragsdale from the NASA Lewis Research Center

REFERENCES

1. Mensing, A. E. and J. S. Kendall: Experimental Investigation of Containment of a Heavy Gas in a Jet-Driven Light-Gas Vortex. United Aircraft Research Laboratories Report D-910091-4, prepared under Contract NASw-847, March 1965. Also issued as NASA CR-68931.

2. Kraver, T. C.: A Study of the Radiation from Argon Plasma. Master of Science Thesis, Department of Aeronautics and Astronautics, M.I.T., February 1961.

3. Gagosz, R. M., J. Waters, F. C. Douglas, and M. A. DeCrescente: Optical Absorption in Fused Silica During TRIGA Reactor Pulse Irradiations. United Aircraft Research Laboratories Report F-910485-1, prepared under Contract NASw-847, September 1967. To be issued as NASA CR report.

4. Douglas, F. C., R. M. Gagosz, and M. A. DeCrescente: Optical Absorption in Transparent Materials Following High Temperature Reactor Irradiation. United Aircraft Research Laboratories Report F-910485-2, prepared under Contract NASw-847, September 1967. To be issued as NASA CR report.

5. Latham, T. S.: Nuclear Criticality Studies of Specific Nuclear Light Bulb and Open-Cycle Gaseous Nuclear Rocket Engines. United Aircraft Research Laboratories Report F-910375-2, prepared under Contract NASw-847, September 1967. To be issued as NASA CR report.

6. McLafferty, G. H. and H. E. Bauer: Studies of Specific Nuclear Light Bulb and Open-Cycle Vortex-Stabilized Gaseous Nuclear Rocket Engines. United Aircraft Research Laboratories Report F-910093-37, prepared under Contract NASw-847, September 1967. To be issued as NASA CR report.

LIST OF SYMBOLS

D	Diameter of coaxial-flow chamber, ft or in.
E	Circumferential electric field, v/cm
H_Z	Axial magnetic field, amp-turns/cm
L_N	Length of chamber from inlet plane to nozzle throat, in. or ft
$\bar{p}$	Average partial pressure of inner-jet gas, lb/ft^2 or atm
P	Total pressure, lb/ft^2 or atm
q	Conduction heat flux, w/cm
r_B	Buffer stream radius at inlet, in. or ft
r_I	Inner-jet radius at inlet, in. or ft
r_o	Peripheral wall radius, in. or ft
T	Absolute temperature, deg K
V_B	Inlet velocity of buffer stream, ft/sec
V_{BAO}	Average inlet velocity of combined buffer stream and outer stream, ft/sec
V_I	Inlet velocity of inner jet, ft/sec
V_O	Inlet velocity of outer stream, ft/sec
z	Axial distance from inlet plane, in. or ft

FIG. 1

COAXIAL-FLOW TEST APPARATUS

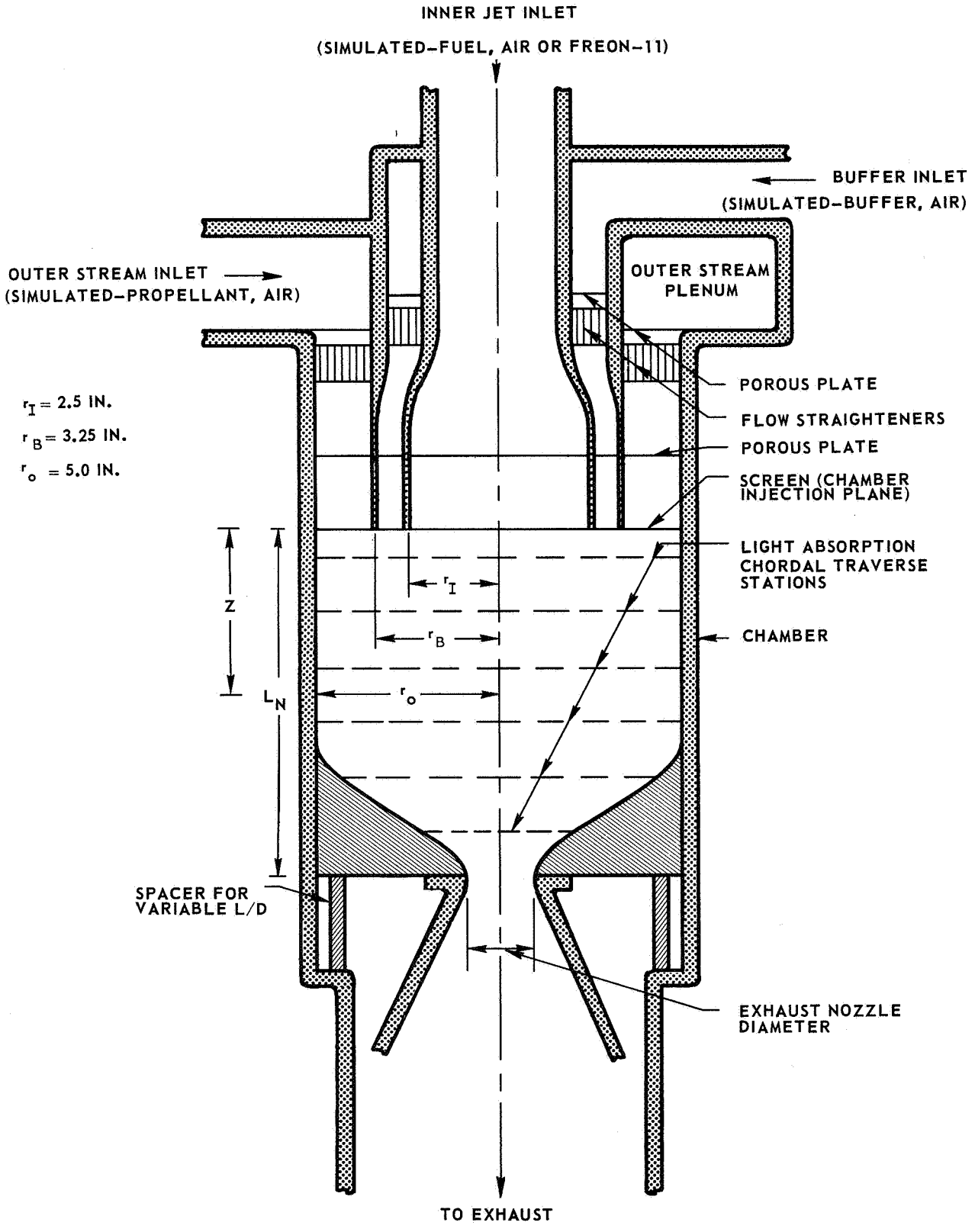

PHOTOGRAPHS OF COAXIAL-FLOW JETS SHOWING EFFECT OF BUFFER GAS VELOCITY RATIO ON CONTAINMENT OF INNER-JET GAS

F-910093-38

V_{BAO}/V_I IS MAXIMUM VALUE FOR WHICH RECIRCULATION COULD BE PREVENTED BY PROPER CHOICE OF BUFFER VELOCITY

AVERAGE OUTER STREAM AND BUFFER STREAM VELOCITY, $V_{BAO} \approx 82$ FT/SEC FOR ALL CONDITIONS
INNER-JET VELOCITY, $V_I \approx 4.1$ FT/SEC FOR ALL CONDITIONS
$V_{BAO}/V_I \approx 20$ FOR ALL CONDITIONS

OUTER STREAM AND BUFFER STREAM GAS – AIR, INNER-JET GAS – FREON-11

INLET CONFIGURATION – $r_I/r_O = 0.5$, $r_B/r_O = 0.65$
CHAMBER LENGTH-TO-DIAMETER RATIO, $L_N/D = 1.25$
EXHAUST NOZZLE DIAMETER AT THROAT – 6 IN.

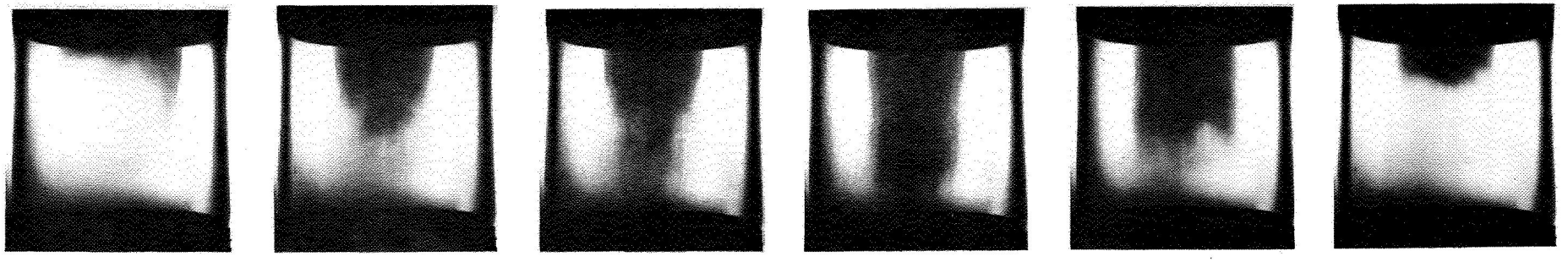

1.0 0.7 0.55 0.4 0.3 0.0

V_B/V_{BAO}

FIG. 2

FIG. 3

EFFECT OF VELOCITY RATIO V_B/V_{BAO} ON CONTAINMENT CHARACTERISTICS OF COAXIAL FLOW JETS FOR V_{BAO}/V_I = 9 AND 18

AVERAGE OUTER STREAM AND BUFFER STREAM VELOCITY, $V_{BAO} \approx 82$ FT/SEC FOR ALL CONDITIONS

OUTER STREAM AND BUFFER STREAM GAS – AIR

INLET CONFIGURATION – $r_I/r_O = 0.5$, $r_B/r_O = 0.65$

CHAMBER LENGTH – TO – DIAMETER RATIO, $L_N/D = 1.25$

EXHAUST NOZZLE DIAMETER AT THROAT – 6 IN.

SYMBOL	INNER–JET GAS	V_{BAO}/V_I	INNER JET GAS VELOCITY, V_I
○—○	AIR	18	4.5
●—●	FREON– 11	18	4.5
△– –△	AIR	9	9.1

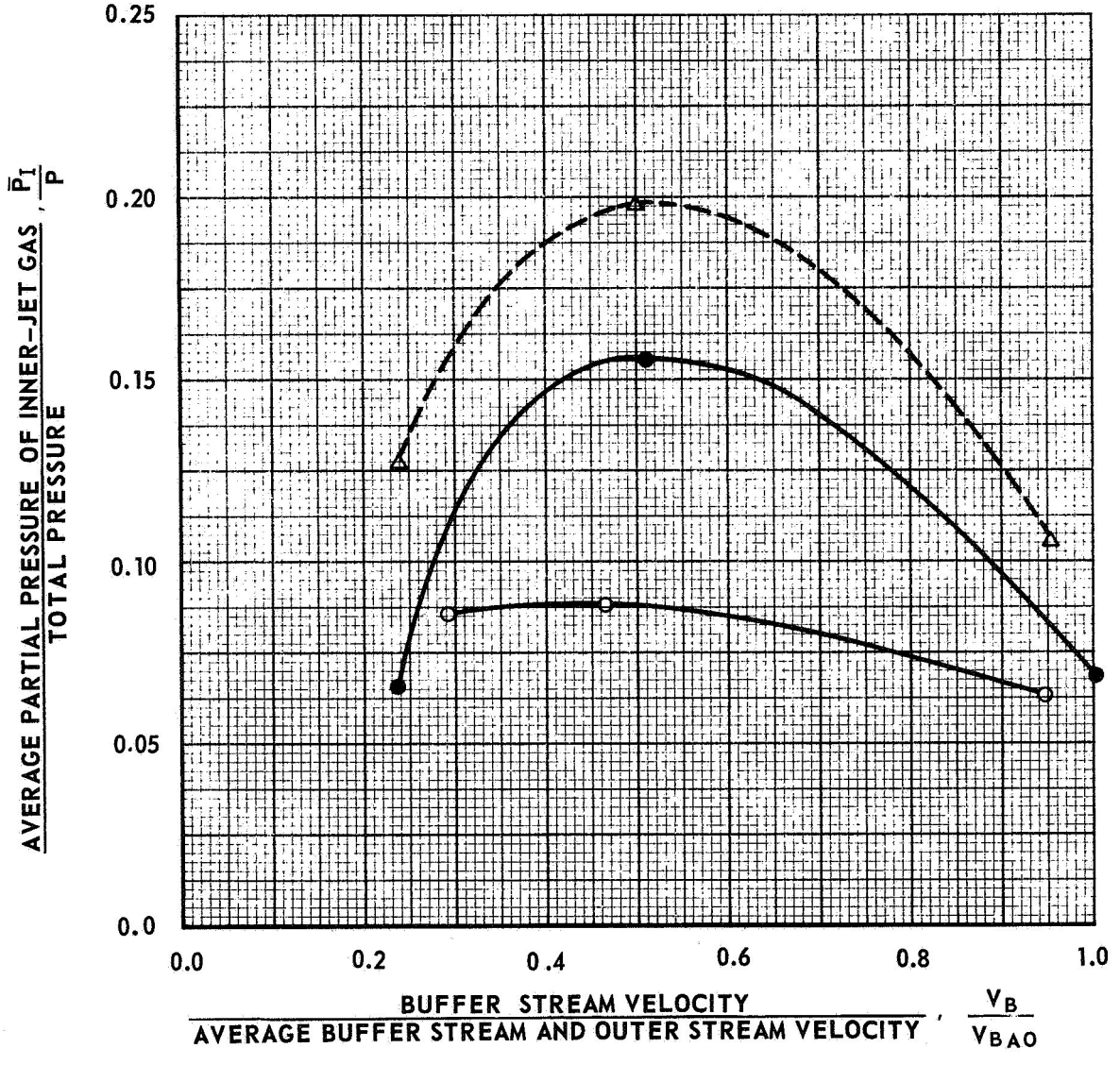

FIG. 4

EFFECT OF CHAMBER L_N/D ON MAXIMUM VALUE OF V_{BAO}/V_I FOR WHICH RECIRCULATION COULD BE PREVENTED BY PROPER CHOICE OF BUFFER VELOCITY

SEE FIG. 2 FOR TYPICAL FLOW VISUALIZATION PHOTOGRAPHS

AVERAGE OUTER STREAM AND BUFFER STREAM VELOCITY, $V_{BAO} \approx 82$ FT/SEC FOR ALL CONDITIONS

OUTER STREAM AND BUFFER STREAM GAS–AIR, INNER JET GAS–FREON–11

INLET CONFIGURATION – $r_I/r_O = 0.5$, $r_B/r_O = 0.65$

EXHAUST NOZZLE DIAMETER AT THROAT – 6 IN.

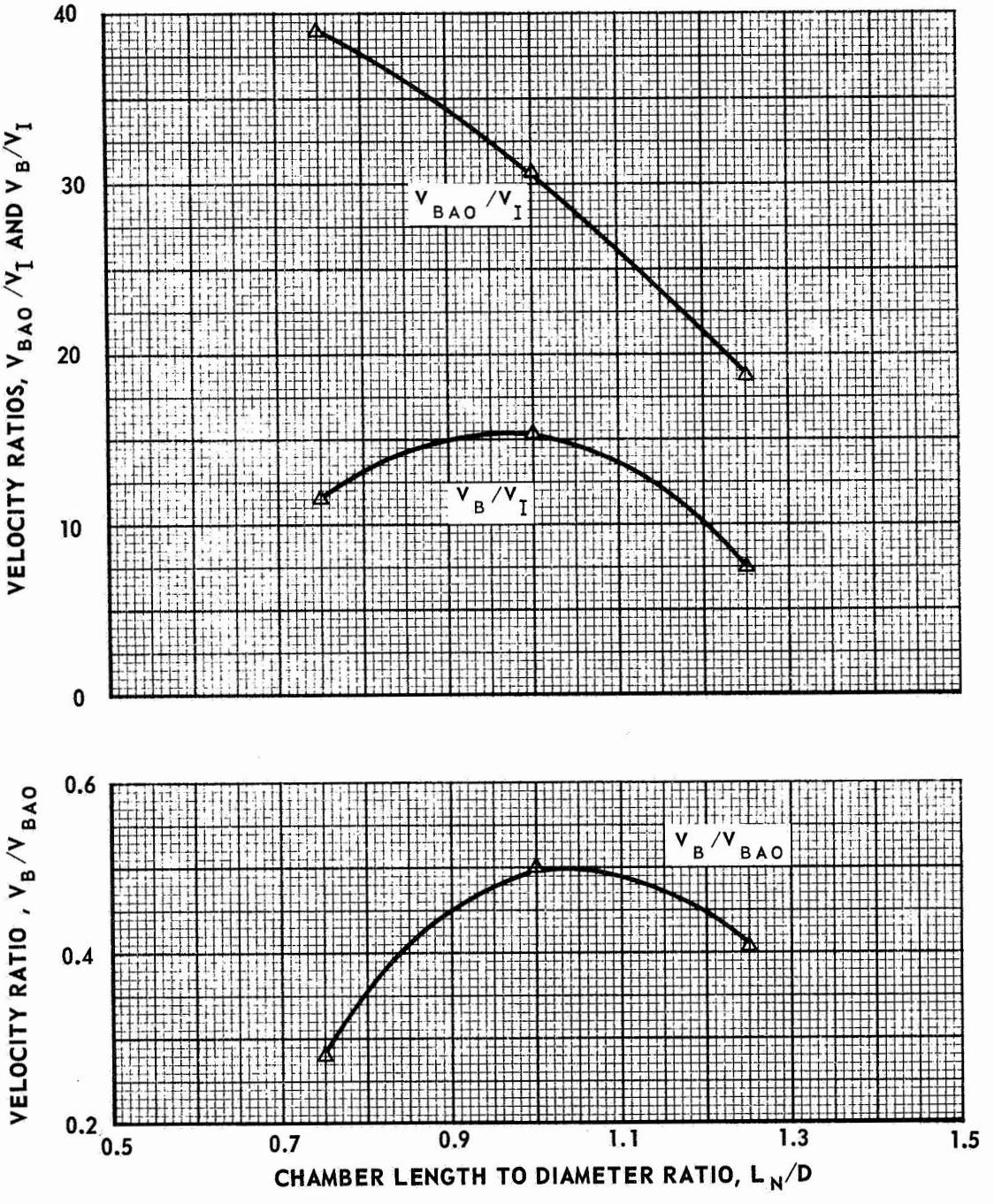

F-910093-38

FIG. 5

SKETCH OF SIMPLE GAS LOAD CONFIGURATION AND PHOTOGRAPH OF ARGON DISCHARGE

a) SKETCH OF CONFIGURATION

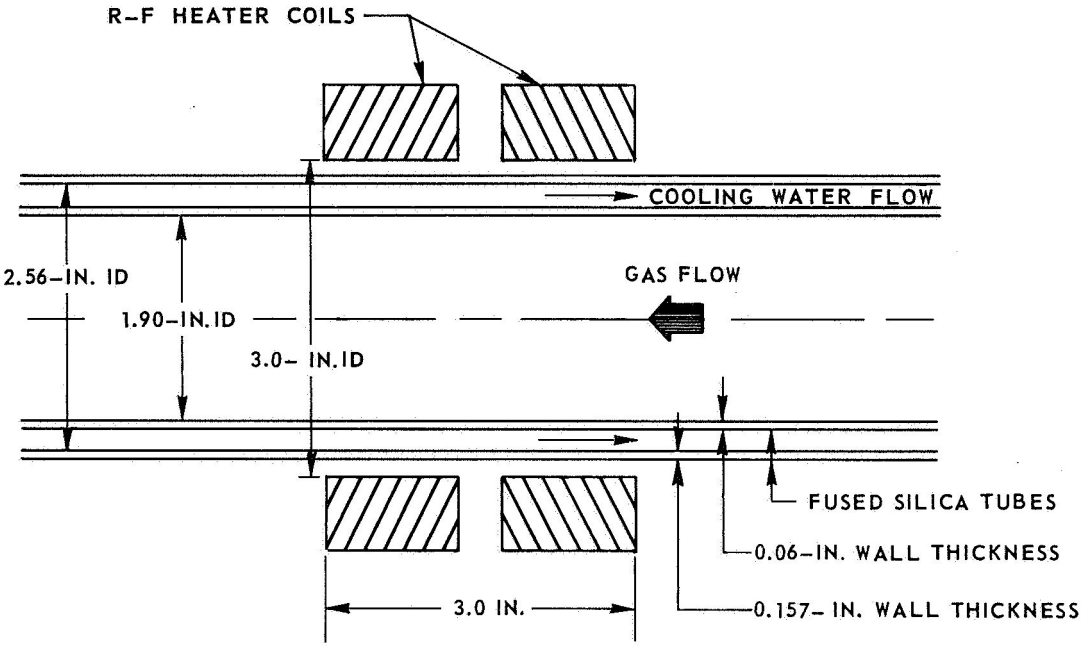

b) PHOTOGRAPH OF ARGON DISCHARGE WITH NO FLOW

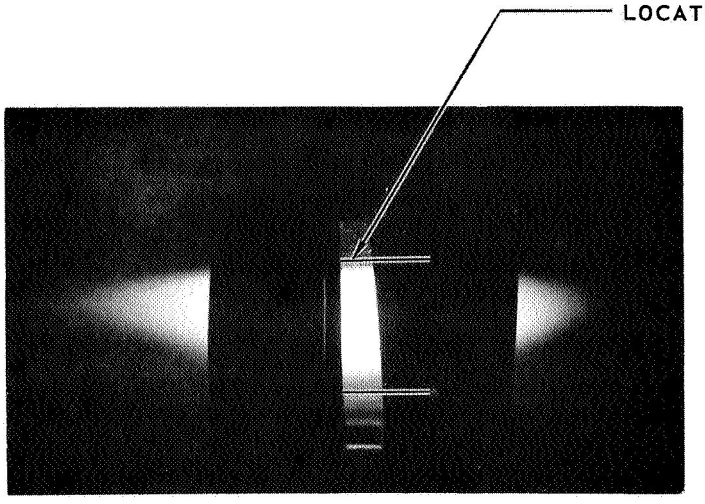

PRESSURE = 1.5 ATM

$$\frac{\text{DISCHARGE DIAMETER}}{\text{INNER TUBE DIAMETER}} \approx 0.7$$

FIG. 6

SKETCH OF SIMPLE GAS LOAD CONFIGURATION WITH SWIRL INJECTION AND PHOTOGRAPH OF ARGON DISCHARGE

a) SKETCH OF CONFIGURATION

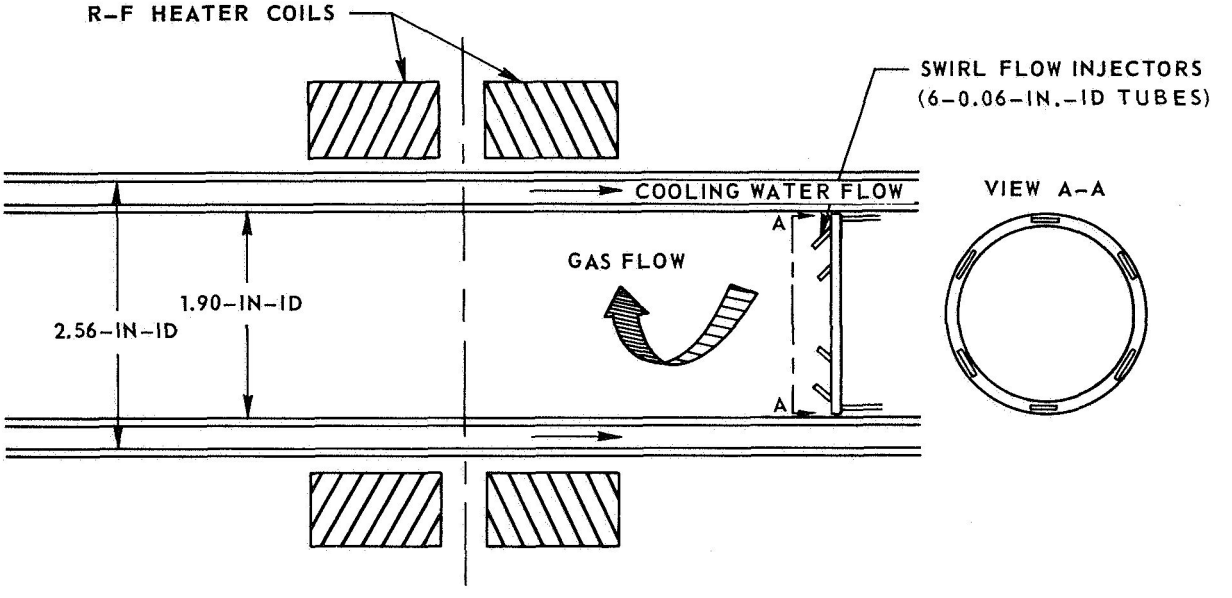

b) PHOTOGRAPH OF ARGON DISCHARGE

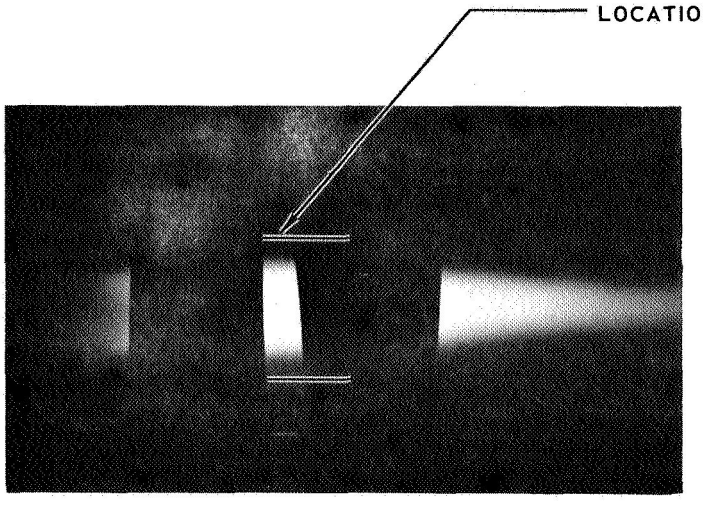

PRESSURE = 1 ATM

$$\frac{\text{DISCHARGE DIAMETER}}{\text{INNER TUBE DIAMETER}} \approx 0.7$$

FIG. 7

SKETCH OF VORTEX CONFIGURATION AND PHOTOGRAPH OF ARGON DISCHARGE

a) SKETCH OF CONFIGURATION

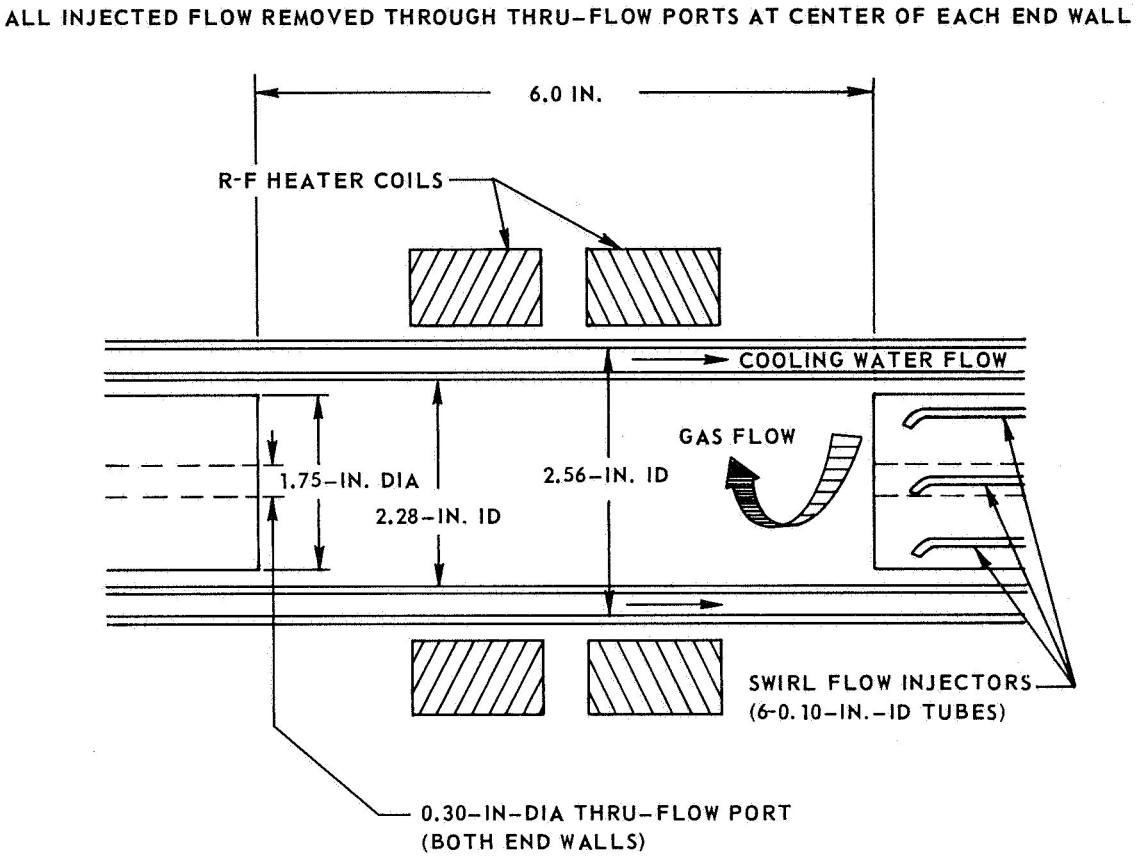

b) PHOTOGRAPH OF ARGON DISCHARGE

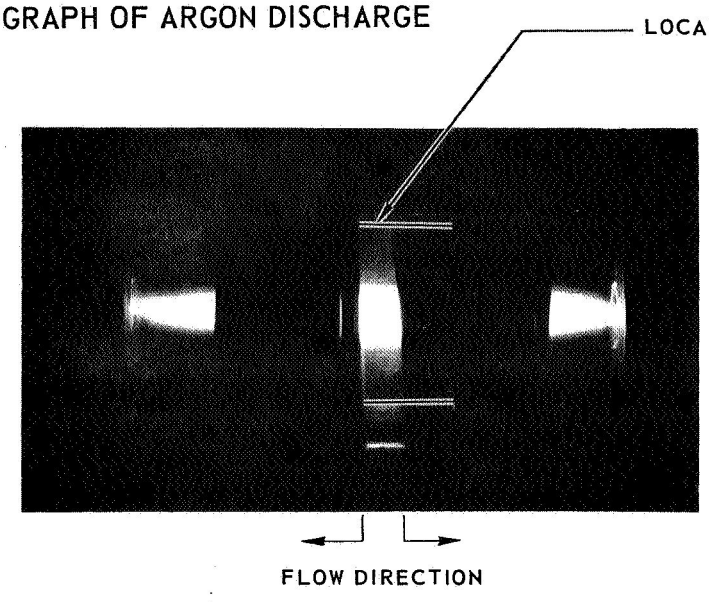

PRESSURE = 1 ATM

$$\frac{\text{DISCHARGE DIAMETER}}{\text{INNER TUBE DIAMETER}} \approx 0.33$$

SKETCHES AND SPECIFICATIONS OF TRANSPARENT – WALL MODEL CONFIGURATIONS

a) AXIAL COOLANT TUBE CONFIGURATION

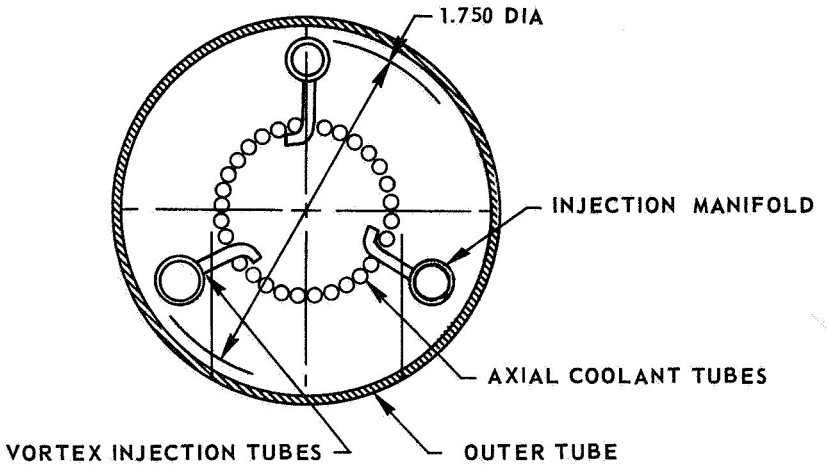

b) CIRCUMFERENTIAL COOLANT TUBE CONFIGURATION

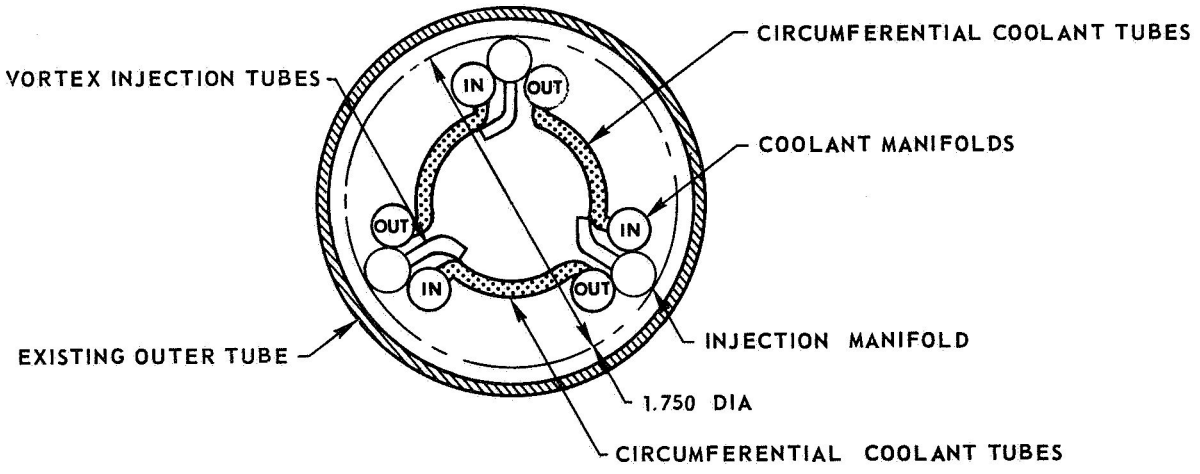

c) SPECIFICATIONS

TRANSPARENT WALL PROPERTIES		PRESENT SPECIFICATION	PROBABLE FUTURE SPECIFICATION
TRANSMISSION WAVELENGTH (Å)	MIN	2800	1600
	MAX	8000	≈30,000
COOLANT TUBE OD (IN.)		0.080	0.040
WALL THICKNESS (IN.)		0.020	0.005
OPERATING TEMPERATURE (DEG C)		800	1100

FIG. 9

SCHEMATIC OF PARTICLE SEEDING SYSTEM

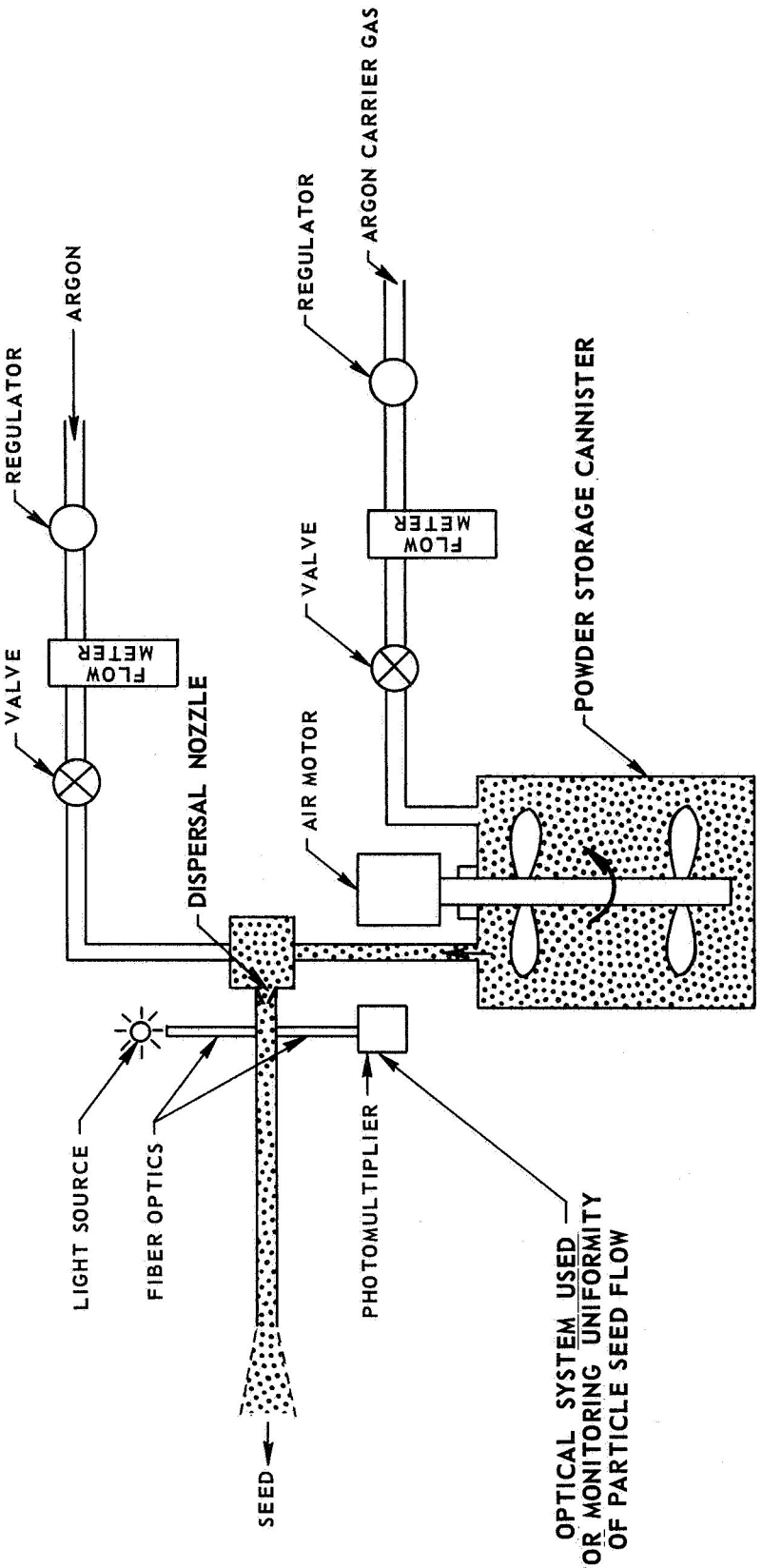

FIG. 10

PHOTOGRAPHS OF R-F DISCHARGE SHOWING CONTRACTION FROM WALLS

ARGON WEIGHT FLOW = 0.0065 LB/SEC
ID OF DISCHARGE TUBE = 92 MM
PRESSURE = 0.8 ATM
POWER IN GAS = 7 KW

a) NORMAL EXPOSURE

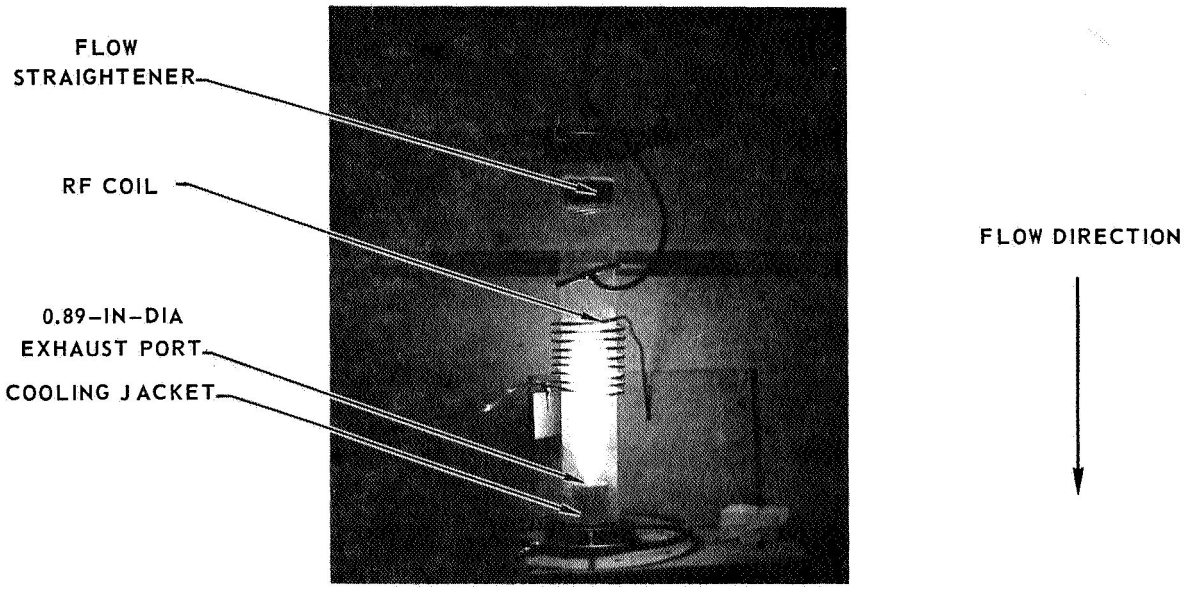

b) EXPOSURE 1/100 OF PHOTO a)

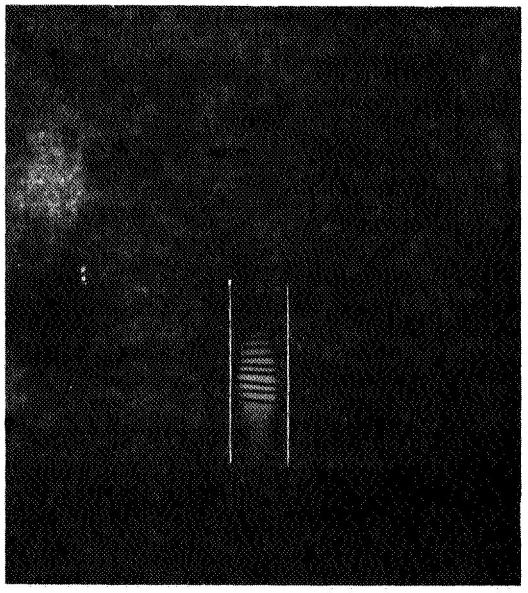

FIG. 11

THEORETICAL RADIAL VARIATIONS OF TEMPERATURE, HEAT FLUX, AND MAGNETIC AND ELECTRIC FIELDS IN AN INDUCTION-HEATED PLASMA

ARGON GAS
PRESSURE = 1 ATM
FREQUENCY, $f = 10^7$ CYCLES/SEC

——— RADIATION ACCORDING TO REF. 1
(TOTAL RADIATION = 47.0 WATTS/CM)

– – – – NO RADIATION